ARCHIVES OF TRANSPORT *ISSN (print):* *0866-9546*
Volume 76, Issue 4, 2025 ***e-ISSN (online):*** *2300-8830*
DOI: *10.61089/aot2025.c3rn0c11*

IMPROVING AERODYNAMIC PERFORMANCE OF INTERMODAL TRAINS THROUGH OPTIMIZATION OF LOADING PLANS

Karol NEHRING[1], Łukasz KISZKOWIAK[2]

[1] *Faculty of Transport, Warsaw University of Technology, Warsaw, Poland*

[2] *Faculty of Mechatronics, Armament & Aerospace, Military University of Technology, Warsaw, Poland*

Abstract:

This paper addresses the improvement of energy efficiency in intermodal freight trains by reducing aerodynamic drag through optimization of container arrangement on railcars. In current terminal practice, loading plans are usually driven by local criteria such as minimizing crane operating time or travel distance, which may result in non-compact cargo configurations and increased aerodynamic losses during train movement. A mathematical model of aerodynamic drag is formulated using position-dependent drag coefficients and a gap-penalty function that reflects the length and location of empty slots in the train consist. The loading problem is modelled as a constrained assignment task with the primary objective of minimizing crane working time. Three approaches to generating the initial loading plan are analyzed: a slot-priority heuristic, a greedy algorithm, and an ant colony optimization algorithm. On this basis, a dedicated post-processing algorithm is applied, which iteratively relocates containers towards the front of the train, reduces gaps between units, and preserves all technical and operational constraints. The method is implemented by linking a FlexSim simulation model of an inland intermodal terminal with Python-based optimization procedures. Nine scenarios with different shares of containers from the road zone and storage yard are evaluated using 16 replications each. The results show that the proposed procedure can reduce estimated aerodynamic drag by approximately 5–9%, at the cost of increased crane operating time. An energy balance comparison indicates that the additional terminal energy consumption is significantly lower than the traction energy savings, confirming that aerodynamic criteria should be explicitly incorporated into train loading strategies.

Keywords: *intermodal train aerodynamic, intermodal train, algorithm, intermodal transport, aerodynamic efficiency*

To cite this article:

Nehring, K., Kiszkowiak, Ł. (2025). Improving aerodynamic performance of intermodal trains through optimization of loading plans. Archives of Transport, 76(4), 137-159. https://doi.org/10.61089/aot2025.c3rn0c11

Contact:
1) karol.nehring@pw.edu.pl [https://orcid.org/0000-0002-0682-8795] – corresponding author; 2) lukasz.kiszkowiak@wat.edu.pl [https://orcid.org/0000-0002-4855-7639]

Article is available in open access and licensed under a Creative Commons Attribution 4.0 International (CC BY 4.0)

1. Introduction

Intermodal transport plays an increasingly important role in global logistics systems, combining different modes of transport and contributing to the efficiency of the supply chain. The development of this form of transport is particularly important in the context of pursuing sustainable transportation. The number of services performed and the number of transported cargo units are continuously increasing.

Along with the increase in the scale of intermodal transport, the requirements concerning its energy efficiency also grow. Intermodal trains travel at high speeds, which means that aerodynamic drag plays an important role in the energy balance. Aerodynamic drag, which increases exponentially with increasing speed, determines energy consumption as well as the safety of transport (Alicke, 2002).

Research indicates that a significant source of increased motion resistance is the configuration of cargo on railcars that is non-optimal in terms of aerodynamics. A non-compact distribution of containers, leaving numerous free spaces, leads to an increase in drag forces and, consequently, increased energy consumption. In extreme cases, improper cargo arrangement may cause even a several-percent increase in the energy demand of a train (Lai et al., 2007). Moreover, the cargo configuration affects train stability, particularly under variable wind conditions and when changing direction of movement (Quazi et al., 2021).

The arrangement of containers on railcars is largely determined by the way the loading process of an intermodal train is organized. Often, the key criterion in planning the loading process is the minimization of the number of reloading operations or the reduction of the travel distance of handling equipment (Kłodawski et al., 2024). Such an approach enables saving time and energy in terminals, but may lead to an unfavorable cargo distribution, and thus to an increase in aerodynamic drag of the train during movement.

Therefore, minimization of energy consumption does not concern only infrastructure or propulsion technologies, but also the cargo configuration itself, which may significantly influence air resistance and transport efficiency.

In the article, based on a review of scientific literature, a method of optimizing cargo arrangement on railcars in the context of aerodynamics was proposed. A mathematical model describing the considered problem was developed. These two elements became the basis for developing an algorithm that enables modification of the loading plan in such a way as to take into account the aerodynamic parameters of the train. Then, a series of experiments was conducted, which made it possible to determine the scale of aerodynamic drag reduction of the train. The influence of the algorithm on the labor intensity of loading operations was also addressed.

2. Literature review

The aerodynamics of an intermodal train set is a key factor influencing the energy efficiency of rail transport. Aerodynamic losses may significantly affect fuel consumption and the stability of the train set in motion. Several key publications are available that address the issue of freight train aerodynamics, and in particular intermodal trains.

The basic relationships between the cargo arrangement on railcars were already described in 2008 (Lai et al., 2008). Research based on the use of a mathematical model made it possible to determine train motion resistance depending on cargo configuration. According to the research, a correct configuration of intermodal cargo on railcars allows saving fuel even up to 27% (Lai et al., 2008; Rickett et al., 2011).

Similar savings are indicated by one of the few publications that refer both to aerodynamics and to the loading process (Lai et al., 2008). The study presented in the publication was based on the analysis of intermodal train movement in the USA. The authors used a linear programming model allowing for the solution of the problem of assigning cargo to locations on the train while taking into account aerodynamic parameters (ALAM, aerodynamic loading assignment model). Apart from the topic of transport in the USA using double-stack container transport, the subject was also addressed by Hungria, Soares and Mendes (Hungria et al., 2019).

The basic approach to measuring the aerodynamic efficiency of an intermodal train is to determine the level of utilization of the available loading space of the train (Lai et al., 2007; Lai et al., 2008). It turns out, however, that two trains with an identical level of loading space utilization may be characterized by visibly different aerodynamic resistance in motion. Resistance is also conditioned by the location of slots without cargo and their size (i.e., their length).

A factor influencing the energy consumption of a train remains also the wind angle of attack –

particularly when travelling along long straight sections of routes (energy consumption) or when dynamically changing direction (train stability) (Flynn et al., 2016; Zhang et al., 2023).
According to the results of research, the longer the gap between cargo units within the train set, the greater the "penalty" costs of aerodynamic losses. Cargo arranged compactly on the train behaves similarly to a single body in motion. In the case of gaps occurring between containers, a disturbance of airflow (dirty airflow) can be observed. Cargo that is located at a distance of 72 ft (approx. 22 meters) or more behaves as separate bodies (Lai et al., 2008; Maleki et al., 2019).
The greatest aerodynamic drag is encountered by the locomotive. Further, the drag decreases gradually up to approximately the tenth railcar, and then, with regular cargo arrangement, remains at a constant level for subsequent cargo units (Lai et al., 2008). This relationship can be described as follows:

$$C_D A(k) = 14{,}85824e^{-0.29308k} + \\ +9{,}86549e^{-0{,}00007k} + 10{,}66914 \quad (1)$$

Where:
$C_D A(k)$ – the aerodynamic drag coefficient for the k-th position in the train consist [ft^2],
k – the position of the cargo in the train consist.
In the case of a sufficiently long gap between cargo units, the following containers after the gap behave like the first element in the train consist and must overcome additional aerodynamic resistance. The literature does not clearly define a formula for the penalty aerodynamic cost resulting from the lack of continuity in the cargo arrangement. Based on the publication (Lai et al., 2008) it can be stated that adjusted factor for gap in the k slot can be describes as:

$$AF(k) = \frac{C_D A(k)}{C_D A(100)} \quad (2)$$

Where:
$AF(k)$ – adjsted factor for k container gap in the train,
$C_D A(k)$ – the aerodynamic drag coefficient for the k-th position in the train consist [ft^2],
$C_D A(100)$ – the aerodynamic drag coefficient for the 100th position in the train consist [ft^2].
The publication by Li et al. (Li et al., 2017) presents a different approach to the problem. The authors focused on a local problem and the relationship between the length of the gap between containers and the aerodynamic drag coefficient was analyzed. Local configurations of containers were taken into account, and two key variables were considered: the front gap size and the rear gap size. The authors included the distances between containers by comparing the length of the gap between cargo units to the width of the railcar. The study is based on tests carried out using a scaled model and a wind tunnel. The importance of this problem was also recognized by Štastniak, Kurčík and Pavlík (Štastniak et al., 2018), where the authors discussed a railcar dedicated to intermodal transport, enabling the reduction of gaps between cargo units.
A similar "local" problem was discussed by Östh and Krajnović (Östh & Krajnović, 2014). The study focuses on the interaction of forces related to airflow acting on a single container railcar. The position of the railcar within the train consist was taken into account. The authors performed measurements using a scaled model of a container railcar with cargo.
A similar method of conducting research as in the two previously discussed publications was applied by Giappino, Melzi and Tomasini (Giappino et al., 2018). The research results correspond to those discussed earlier.
Earlier research can be supplemented with results presented by Flynn, Hemida and Baker (Flynn et al., 2016). The authors included the influence of crosswinds on the aerodynamics of the train. The results of the study showed that greater airflow disturbances occur on the leeward side of the train. The strongest wind gusts were observed at the front of the train consist.
More modern methods used in studies of aerodynamic phenomena related to the movement of container trains utilize Computational Fluid Dynamics (CFD) and 3D modelling (Arsene & Spiroiu, 2024).This once again allows the determination of how cargo arrangement on railcars affects aerodynamic drag. The authors again refer to two key aspects: energy and safety.
Some authors decided to develop methods that may also be applied in dynamically changing real working conditions. The study by Lai et al. (Lai et al., 2007) is based on a machine vision MV system, which automatically scans passing trains, detects gaps between cargo units and calculates the aerodynamic coefficient, enabling intermodal terminals to

optimize the cargo arrangement. The machine vision method was also used in other publications (Rickett et al., 2011).

Another method that can be used in practice was described by Quazi et al. (Quazi et al., 2021).

As part of the study, a 48-foot container was equipped with surface pressure sensors. Measurements were taken for its different positions in the train consist. The results showed that the aerodynamic drag coefficient differed significantly from laboratory measurements (by even up to 50%), and crosswind conditions had a significant impact on the forces. The analysis of the asymmetry of pressure distribution may serve as an accurate method of assessing the influence of wind on the aerodynamics of trains (Quazi et al., 2021; Yang et al., 2017). Selected publications also refer to other aspects directly related to aerodynamics. One of them is, for example, the relationship between the type of intermodal cargo and the aerodynamic forces acting on it (Opala, 2021). This issue applies not only to intermodal transport (Huo et al., 2021). The significance of aerodynamics is so substantial that it is relevant not only for intermodal train consists travelling at high speeds, but also, for example, for container ships (Deng et al., 2022; Majidian & Azarsina, 2018). Numerous studies have also led to attempts at practical implementation of intermodal cargo units characterized by better aerodynamic parameters than standard intermodal units (Öngüner et al., 2020). The literature review indicates that the aerodynamics of an intermodal train consist has a significant impact on the energy efficiency of transport. Key factors affecting aerodynamics include:

- gaps between cargo units (length and position in the consist),
- empty railcars – especially at the front of the consist,
- the impact of crosswinds on the consist,
- the degree of utilization of loading space.

Despite the fact that authors often draw attention to the relationship between the loading process of the train consist and its aerodynamics, the most common optimization criterion for the loading process is still local savings based on the reduction of the operating time of handling equipment (Nehring et al., 2021; Ng Man Wo & Talley, 2020). However, when comparing the savings obtained in the loading process, it turns out that they may be significantly smaller than the savings at the stage of transporting cargo between terminals.

Authors have so far used various methods in the optimization of loading intermodal train consists:

- simple heuristics (Kłodawski et al., 2024),
- greedy algorithm (Kłodawski et al., 2024),
- genetic algorithm (Li & Zhu, 2019; Said & El-Horbaty, 2015),
- local search heuristics (Heggen et al., 2018),
- Branch and Bound (Heggen et al., 2018),
- linear programming (Dotoli et al., 2013; Dotoli et al., 2015),
- myopic search procedure (MSP) (Kellner et al., 2012),
- simulated annealing (SA) (Kellner et al., 2012).

In the most recent scientific studies, an ant colony algorithm has also been used to optimize this process (Nehring, 2024).Regardless of the method used, the priority is usually to minimize the number of operations carried out by handling equipment, minimize crane working time (or distance), or reduce energy consumption at the loading stage. This is an appropriate approach when considering the loading process itself. Only a broader view of the entire transport process allows one to understand the essence of aerodynamics and its importance for the execution of the whole process.

Despite the increasing interest in the issue of aerodynamics in intermodal transport, further research integrating aerodynamic models with loading optimization algorithms is necessary. Their development may contribute to significant energy savings and improved train consist stability in motion.

3. Characteristics of the analyzed problem

For the purposes of the analyzed problem, the following assumptions were adopted:

- The loading of the train is carried out in a land-based intermodal terminal, in which containers are located in two functional zones:
  - road zone – originating from arrival by road transport. Containers in a single layer and a single row,
  - storage yard – containers located further from the tracks, stored in multiple rows and often in multiple layers.
- The loading is carried out using a single RMG gantry crane;

– Empty railcars awaiting loading are located in the track zone.

The scheme of the terminal is presented in Figure 1. The share of containers originating from particular zones depends on the analyzed variant of the study. Similarly, the method (algorithm) of crane operation. After positioning the train at the terminal, the loading process begins, and the containers assigned for loading, in accordance with the established order, are placed on railcars in their dedicated slots. The loading is carried out in simple cycles by the crane. The process must respect all constraints described later in point 4.

The loading sequence is carried out in accordance with the loading plan. The loading plan is determined using one of the algorithms presented in Chapter 5.

4. Mathematical model

Unfortunately, equation (1) described in the publication (Lai et al., 2008) does not refer to the actual lengths of intermodal units, but only to the position of the container in the train consist. It is only possible to estimate the penalty cost resulting from the aerodynamic gap by assuming that after a sufficiently long gap between railcars occurs (the aerodynamic drag after a gap longer than, for example, 22 m increases to that corresponding to the first unit at the front of the train consist). Taking into account data from other publications, it can be assumed that the additional aerodynamic drag caused by an empty slot s will amount to (Lai et al., 2008):

$$C_D A\big(s, G(s)\big) = C_D A(s) + \left(C_D A_{max} - C_D A(s)\right) \cdot \left(1 - e^{-\alpha G(s)}\right) \quad (3)$$

Where:
$C_D A(s)$ – baseline aerodynamic drag for the slot s,
$C_D A_{max}$ – maximum aerodynamic drag for the slot (aerodynamic drag of the first unit in the train consist),
$1 - e^{-\alpha G}$ – dimensionless penalty coefficient for the gap in the consist,
$G(s)$ – gap length between containers normalized by the railcar width:

$$G(s) = \frac{L(s)}{B} \quad (4)$$

$L(s)$ – slot length s [m]
B – railcar width [m]
α – calibration coefficient.

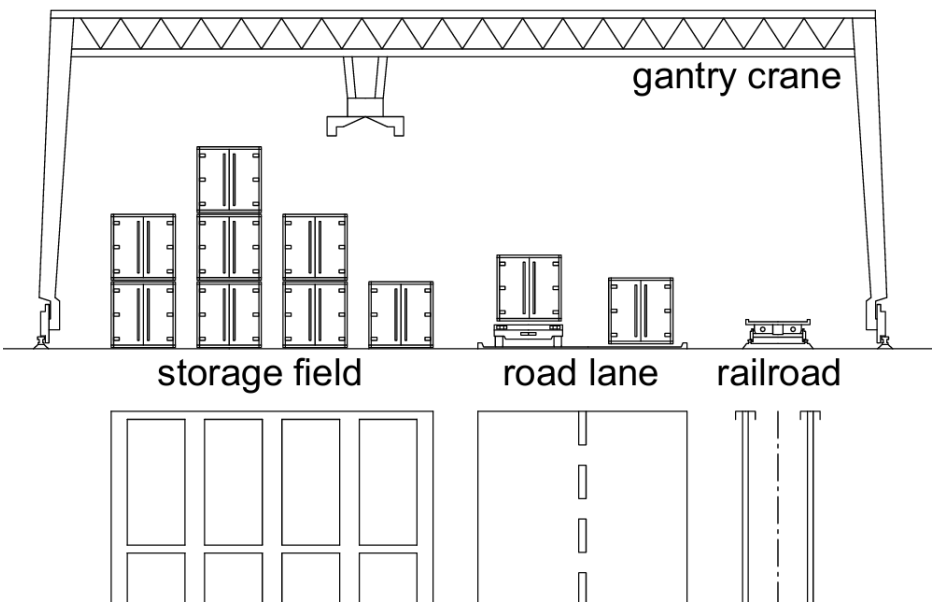


Fig. 1. Analyzed layout of the intermodal terminal. Source: own elaboration

The coefficient α constitutes a calibration parameter of the aerodynamic penalty function. It was assumed that a gap equal to the width of the railcar (i.e., G = 1) causes approximately a 60% increase in drag relative to the compact configuration, which corresponds to the value $\alpha \approx 0.92$. This assumption is consistent with qualitative aerodynamic research results describing a rapid increase in drag for small gaps between containers (Li et al., 2017; Mosca et al., 2018). The total aerodynamic drag of the consist (estimated as the sum of $C_D A$ of cargo units including penalties for gaps) can be expressed as:

$$C_D A(train) = \sum_{s \in \boldsymbol{S}} C_D A(s, G(s)) \tag{5}$$

Where:
$\boldsymbol{S}$ – set of slots on the serviced railcars, $\boldsymbol{S}$ = {1, …, *s*, …., *S*}
The total aerodynamic drag is calculated for loading solutions of the train consist obtained as a result of the operation of the selected crane algorithm. In the mathematical loading model, the objective criterion function is used as follows:

$$\boldsymbol{F}(Z) = t_{load} = \sum_{c \in \boldsymbol{C}} \sum_{s \in \boldsymbol{S}} \sum_{r \in \boldsymbol{R}} z_{csr} \cdot t_{o(csr)} \rightarrow min \tag{6}$$

Where:
$\boldsymbol{C}$ – set of containers to load, $\boldsymbol{C}$ = {1, …, *c*, …., *C*},
C – number of containers to load,
$\boldsymbol{R}$ – set of serviced railcars, $\boldsymbol{R}$ = {1, …, *r*, …, *R*}
R – number of serviced railcars
$\boldsymbol{S}$ – set of slots on the serviced railcars, $\boldsymbol{S}$ = {1, …, *s*, …., *S*}
S – number of slots on the railcars to be serviced
$t_{o(csr)}$ – service time of container *c* assigned to slot *s* on railcar *w*
z_{csr} – decision variable z_{csr} assigning the container to the selected slot on the railcar of the train:

$$z_{csr} = \begin{cases} 1, & f\ container\ c \text{ is assigned to slot} \\ & \text{on the railcar } r \\ 0, & \text{in the remaining cases} \end{cases} \tag{7}$$

The service time $t_{o(csr)}$ depends on factors such as (Nehring, 2024):
– the travel time of the crane to container c from the slot where container (c–1), serviced prior to container c, was placed,
– the coordinates of container c and slot s,
– the location of container c,
– the stacking level of container c,
– the number of containers placed above container c,
– the parameters of handling equipment.
The details of determining the service time of containers were described, among others, in (Kłodawski et al., 2024) and (Nehring, 2024). In addition, in order to correctly account for constraints for the loading process of the train consist, the following conditions must be considered:

1. Each container c may be assigned to at most one slot s:

$$\forall c \in \boldsymbol{C} \quad \sum_{s \in \boldsymbol{S}} \sum_{r \in \boldsymbol{R}} z_{csr} \leq 1 \tag{8}$$

2. The length type of container c assigned to slot s must be consistent with the size of the selected slot:

$$\forall c \in \boldsymbol{C} \quad \forall s \in \boldsymbol{S} \quad \forall r \in \boldsymbol{R} \qquad z_{csr} = 1 \rightarrow L \tag{9}$$

Where:
L_c – container length type *c*
L_r – total length of the railcar *r*

3. The total length of slots assigned to railcar r may not exceed the total length of that railcar:

$$\forall r \in \boldsymbol{R} \quad \sum_{s \in \boldsymbol{S}(r)} L_s \leq L_r \tag{10}$$

Where:
L_s – slot length *s*

4. The total length of containers assigned to railcar r may not exceed the length of that railcar:

$$\forall c \in \boldsymbol{C} \quad \sum_{s \in \boldsymbol{S}} \sum_{r \in \boldsymbol{R}} z_{csr} \cdot L_c \leq L_r \tag{11}$$

5. The total weight of containers assigned to railcar r may not exceed the load limit for the railcar:

$$\forall r \in \boldsymbol{R} \quad \sum_{c \in \boldsymbol{C}} \sum_{s \in \boldsymbol{S}(r)} z_{csr} \cdot M_c \leq M_r^{max} \tag{12}$$

Where:
M_c – weight of the *c*-th container,
M_r^{max} – maximum allowable load of the railcar *r*.

6. The total weight of containers placed on the train should not exceed the permissible load specified for the train consist:

$$\sum_{c\in \boldsymbol{C}}\sum_{s\in \boldsymbol{S}}\sum_{r\in \boldsymbol{R}} z_{csr}\cdot M_c \le M_{train}^{max} \quad (13)$$

Where:
M_{train}^{max} – maximum allowable weight of the train consist

7. The axle load (front and rear) of each railcar must not be exceeded:

$$\forall r \in \boldsymbol{R} \qquad M_{r(b1)} \le M_{r(b1)}^{max}, \qquad M_{r(b2)} \le \quad (14)$$

$M_{r(b1)}$ – maximum allowable load for the front axle of the railcar *r*,
$M_{r(b1)}^{max}$ – maximum allowable load for the rear axle of the railcar *r,*
$M_{r(b2)}$ – calculated load for the front axle of the railcar *r,*
$M_{r(b2)}^{max}$ – calculated load for the rear axle of the railcar *r.*

8. The load on the front and rear axle of the railcar may not exceed the ratio 3:1:

$$\forall r \in \boldsymbol{R} \qquad \frac{1}{3}M_{r(b2)} \le M_{r(b1)} \le 3M_{r(b2)} \quad (15)$$

The calculation of axle loads is based on the lever principle (Bruns & Knust, 2012). The geometric centre is assumed as the centre of gravity of the container. The support points of the railcar are the points where the bogies are connected to the railcar frame. In the case where the railcar has more than one axle, this condition must be verified for each axle pair.
It must be emphasized that the aerodynamic drag model used in this study represents relative variation rather than absolute traction demand. The penalty function incorporates gap length normalized by railcar geometry and monotonically increases drag for longer discontinuities, which reflects qualitative findings from aerodynamic studies. The model does not include crosswind turbulence effects, Reynolds-scale flow transitions or changes in boundary layer separation along the consist. For this reason, the obtained values should be interpreted as relative aerodynamic differences between loading configurations rather than absolute physical drag values.

5. Measurement method

5.1. Loading algorithms for the train consist

To determine the initial loading plan for the train consist, three computational approaches differing in the method of determining the service order of containers and their assignment to slots were applied. These algorithms allow the reproduction of various operating strategies of handling equipment used both in terminal practice and in simulation studies. For research purposes, three algorithms were used:

– **Algorithm 1 (slot priority)** is based on the principle of servicing subsequent slots in the train consist. Moving from the front of the train consist, the crane collects containers and places them in slots starting from the first to the last. The first suitable available container, counting from the front, is placed in the slot. After placing one container, the algorithm proceeds to handle the next element of the list. The block diagram of the algorithm is presented in Figure 2.a.
– **Algorithm 2 (greedy algorithm)** is based on the principle of local minimization of crane travel time. At each step, the container closest to the current position of the crane is selected, and then—after picking it up—the nearest available slot in the train consist to which the container can be assigned is selected. After placing the cargo, the algorithm updates the crane position and repeats the procedure until all containers are handled (Figure 2.b).
– **Algorithm 3 (ant colony algorithm)**, applied in the train loading model, generates a sequence of assignments of containers to slots, minimizing the total working time of the crane. Each agent (ant) constructs a solution by moving between graph vertices representing containers and slots. The probability of selecting a given transition depends on:
  - pheromone trails reflecting the quality of solutions,
  - a distance heuristic related to the time of travelling a given segment of the route.

After generating all paths, the best solution updates the pheromone level, strengthening preferences for short and efficient crane routes. The process iteratively repeats solution construction, pheromone evaporation, and pheromone reinforcement until a stable, optimized loading plan is obtained (Figure 3). Table 1 presents the parameters of the ant colony algorithm for which the best results were obtained.
The details of parameter selection for the ant colony algorithm were described in (Nehring, 2024). Each of the approaches generates a complete loading plan, which is then evaluated in terms of the operation execution time and the aerodynamic parameters of the consist. Only after that does the algorithm improving aerodynamic parameters begin its operation, and after completing its work the results are compared again. This makes it possible to determine the potential improvement of the solution in the context of aerodynamics, as well as to analyze the impact of introducing adjustments in the loading plan on the total process execution time.

5.2. Algorithm for improving aerodynamic parameters

The algorithm that modifies the arrangement of containers on railcars (for improving aerodynamic parameters) aims to reduce the aerodynamic drag of the consist by achieving the most compact cargo configuration possible. Its operating logic is based on iterative searching of the initial loading plan for containers that can be moved closer to the front of the train without violating technical constraints. The process begins with the calculation of the current indicators — the estimated aerodynamic drag and the total crane operating time resulting from the current loading plan. Then, the algorithm goes through the list of containers, considering them from the last to the first. For each container, the possibility of moving it to the first available free slot located closer to the front of the consist is checked. If the move is possible, the container is transferred. The procedure continues until all containers have been analyzed or until there are no free slots left in the consist that can be used.

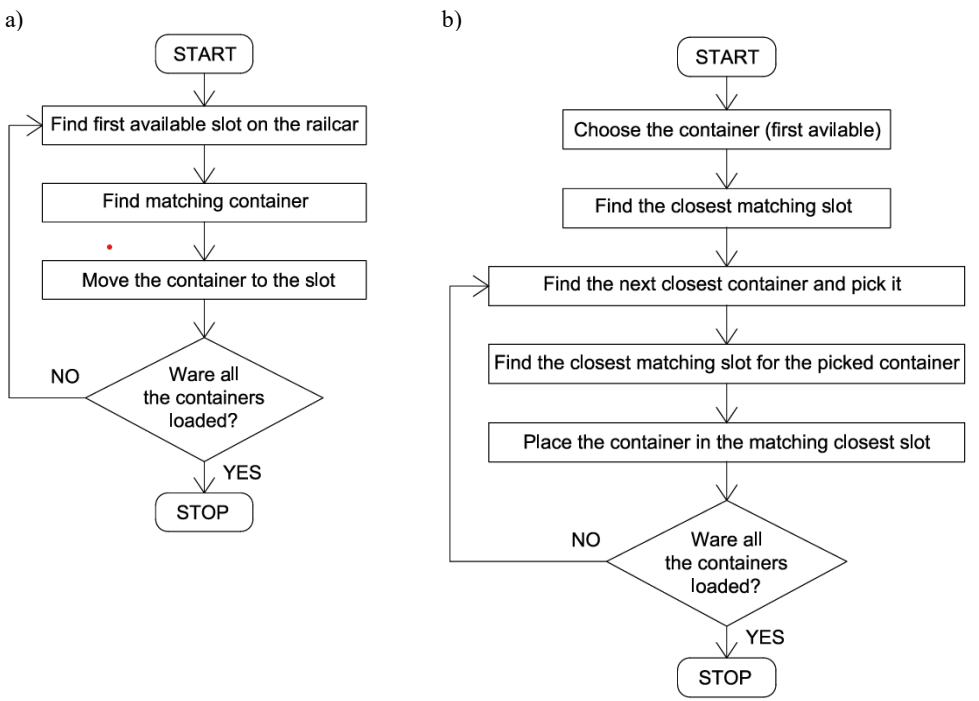


Fig. 2. Block diagram of algorithms 1–3: a) slot priority algorithm; b) greedy algorithm. Source: own elaboration

```
START
// Initialization
initialize_pheromone_levels()
initialize_parameters()    // α, β, ρ, number of ants, number of iterations
FOR iter = 1 TO max_iterations:
   FOR each ant k:
      solution_k = empty_solution()
      WHILE exists_unassigned_containers():
         c = select_container_based_on_probability(pheromone, heuristic)
         s = select_slot_based_on_probability(pheromone, heuristic)
         assign_container_to_slot(c, s, solution_k)
      ENDWHILE
      evaluate_solution(solution_k)    // crane time, route quality
   ENDFOR
   best_solution = choose_best_solution()
   update_pheromone_levels(best_solution, evaporation_rate = ρ)
ENDFOR
return best_solution
STOP
```

Fig. 3. Pseudocode of the ant colony algorithm. Source: own elaboration

Table 1. Parameters of the ant colony algorithm. Source: own elaboration

Parameter	Value
Number of the ants (agents)	100
Number of iterations	10
Pheromone evaporation coefficient	0,5
Pheromone weight coefficient	1
Heuristic weight coefficient	2
Exploration coefficient	100

The final arrangement of containers and the values of the calculated aerodynamic parameters are recorded as the result of the algorithm. Thus, the algorithm aims to achieve improvements in three aspects:

- minimization of the number of empty slots (particularly at the front of the train consist),
- minimization of the gap lengths between containers in the train consist,
- compact arrangement of cargo on the railcars.

The algorithm written in pseudocode form is presented in Figure 4.

5.3. Simulation studies of the process

The simulation method was selected due to the complexity of the train consist loading process, the dependence of operation times on the spatial layout of the terminal, and numerous interactions between the crane and the changing container configuration. Simulation allows for a realistic representation of the operation of handling equipment, taking into account their movement parameters and assessing the impact of the adopted algorithm on the duration of operations.

The FlexSim environment enables detailed modelling of crane movement and container flow, but does not provide tools for advanced optimization using, for example, an ant colony algorithm. For this reason, the simulation model was integrated with Python code, which was responsible for implementing the optimization and computational algorithms, allowing the combination of simulation realism with computational flexibility.

```
START
  // Data input
  load_loading_plan()

  // Calculation of initial indicators
  drag = calculate_aerodynamic_drag(loading_plan)
  dist = calculate_gantry_travel_distance(loading_plan)

  // Iteration over all containers (from the end)
  WHILE exists_unchecked_containers():

    c = get_last_unchecked_container()

    IF can_be_moved_closer_to_front(c) == TRUE THEN

      // Identification of the first free slot from the front
      s = find_first_empty_slot_from_front_that_fits(c)

      // Container transfer
      place_container_in_slot(c, s)
      update_loading_plan()

      // Update of indicators
      drag = calculate_aerodynamic_drag(loading_plan)
      dist = calculate_gantry_travel_distance(loading_plan)

      // If no free slots remain, terminate
      IF no_empty_slots_remaining() == TRUE THEN
        save_results(loading_plan, drag, dist)
        STOP
      ENDIF

    ENDIF

    mark_container_as_checked(c)

  ENDWHILE

  // Recording of final results
  save_results(loading_plan, drag, dist)
STOP
```

Fig. 4. Loop of the algorithm for improving aerodynamic parameters. Source: own elaboration

The optimization method algorithm includes the following steps:

Step 1. Determination of input data

The necessary parameters are determined, including, among others, the spatial layout of the terminal (functional zones, size and capacity of zones, location of zones), data regarding slots on railcars and containers. Research scenarios and the number of iterations are also established.

Step 2. Random generation of initial loading conditions of the train consist

Random data are generated:

– list of containers to be picked up,
– arrangement of container slots on the railcars.

Step 3. Solution using the selected algorithm (minimization of crane operating time).

To find the initial solution, the method of servicing consecutive containers, the greedy algorithm, or the ant colony algorithm was further used (depending on the variant). The algorithms minimize the loading time by the equipment. The results of their operation are a loading plan including information on:

– assignment of cargo to slots on the railcars,
– order of handling cargo.

Step 4. Calculation of the solution parameters from Step 3.

For the base solution, the following indicators are calculated:

– loading execution time t_{load},
– estimated aerodynamic resistance indicator $C_D A(train)$.

Step 5. Export of data sets for the optimization algorithm.

The data on the loading plan from **Step 3** are exported as input data for the optimization algorithm implemented in Python.

Step 6. Operation of the algorithm reconfiguring the container arrangement (minimization of the aerodynamic drag of the train consist).

In the subsequent steps, the algorithm checks possible changes in the loading plan to achieve a cargo arrangement on the railcars with improved aerodynamic parameters.

Step 7. Update of the loading plan and parameter values.

Update of the solution obtained in **Step 3** and recalculation of the loading time t_{load} and the aerodynamic drag indicator $C_D A(train)$.

Step 8. Recording of results.

Recording of results in a form enabling further analysis (e.g., CSV file).

Step 9. Checking the number of iterations.

If the target number of iterations has been reached, proceed to **Step 9**. Otherwise, return to **Step 2.**

Step 10. Analysis of results.

Statistical data are calculated (mean, median, standard deviation, upper and lower quartiles). The analysis of results includes loading time before and after changes, the aerodynamic drag indicator, and a comparison of results for different algorithms and research scenarios.

Step 11. Stop.

The steps of the algorithm, including the integration of the FlexSim environment and Python, are presented in the block diagram in Figure 5.

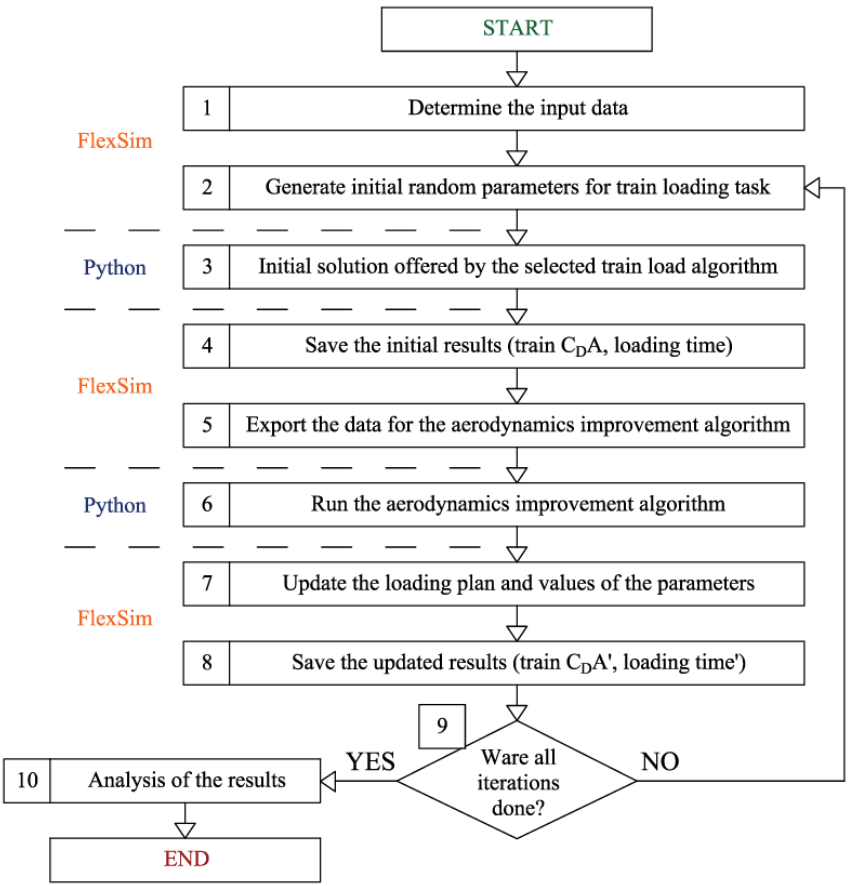


Fig. 5. Loop of the optimization method algorithm. Source: own elaboration

The simulation model was developed in the FlexSim simulation environment, version 2023 (Update 2). It reflects the basic objects comprising a typical inland intermodal terminal, namely:

1. a gantry crane,
2. a track section with railcars prepared for loading,
3. a storage lane for containers ready for loading,
4. a container storage yard with a total length of 525 m and three storage rows.

Proper functioning of the model is ensured through the appropriate definition of loading process methodologies (Figure 6), which were implemented as algorithms using Process Flow and the FlexScript language.

For the purposes of the simulation study, the following assumptions were adopted:

- Loading is performed using an RMG crane;
- The train capacity is 90 TEU (30 railcars);
- The railcars were assigned the following parameters:
  - permissible gross weight: 80,000 kg (for track class C),
  - permissible load: 58,000 kg (for track class C),
  - permissible axle load: 20,000 kg,
  - tare weight of the railcar: 22,000 kg;
- The containers selected for loading were chosen so as not to exceed the maximum permissible gross weight of the train (this condition is additionally verified by model constraints and the algorithm);
- Three types of containers circulate in the system: 20 ft (1C, TEU), 30 ft (1B), 40 ft (1A);
- Each container in the simulation model was assigned a mass, assuming that the maximum permissible weight for each container type cannot exceed 20,320 kg for 1C, 25,400 kg for 1B, and 30,480 kg for 1A;
- For each container, the exact weight was assigned individually and randomly within the allowable range. The lower bound for the weight of any container was assumed to be 5 tons.

The crane parameters are presented in Table 2.

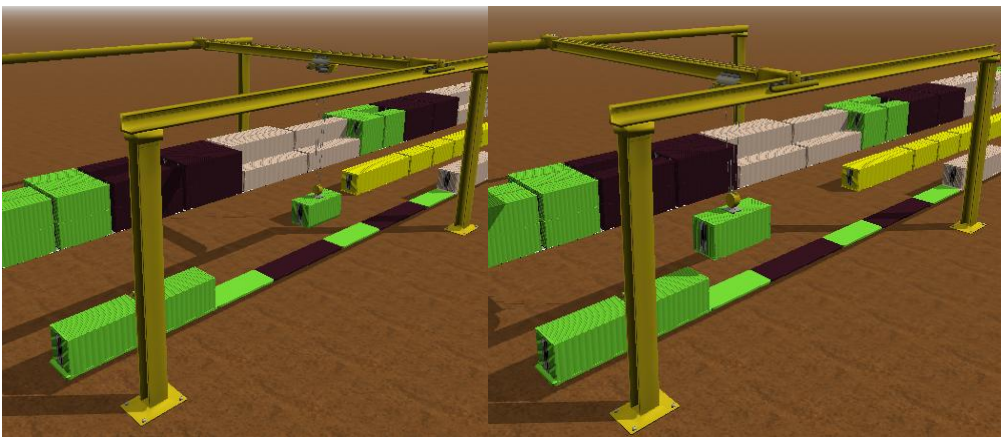


Fig. 6. View of the simulation model – train loading process. Source: own elaboration

Table 2. Crane operating parameters (elementary activity durations). Source: own elaboration

Activity	Value	Unit
Container gripping by the crane	5	s
Container release by the crane	10	s
Crane travel speed	2	m/s
Trolley travel speed	2	m/s
Container lifting speed	0.43	m/s
Container lowering speed	0.43	m/s

6. Research results

6.1. Scenarios of the loading task

The main factor determining the arrangement of containers on the railcars was identified as their pick-up location in the terminal. The distribution of containers directly determines the crane operation method and the order in which they are picked up. During the study, different scenarios of the train consist loading process were analyzed. The individual scenarios differ from each other in:

- the algorithm used to minimize loading time,
- the share of cargo originating from the storage yard in the loading,
- the share of cargo originating from the road zone in the loading.

A total of nine extreme scenarios were analyzed. For each variant, two sets of results were obtained, serving as the basis for further analyses:

1. Data set before improving aerodynamic parameters (operating time of handling equipment and aerodynamic drag),
2. Data set after improving aerodynamic parameters (operating time of handling equipment and aerodynamic drag),

A detailed description of the variants is presented in Table 3.

Table 3. Research scenarios analyzed during the study. Source: own elaboration

Research scenario	Algorithm	Share of cargo from the storage yard [%]	Share of cargo from the road zone [%]
1A	Slot priority	0	100
1B	ACO	0	100
1C	Greedy	0	100
2A	Slot priority	50	50
2B	ACO	50	50
2C	Greedy	50	50
3A	Slot priority	100	0
3B	ACO	100	0
3C	Greedy	100	0

6.2. Results

In the study, the train loading time was adopted as the primary variable determining the quality of the compared algorithms. This parameter directly reflects the operating mode of the transshipment equipment and the resulting arrangement of containers on the railcars, which in turn affects the aerodynamic characteristics of the analyzed trainset.

Based on preliminary (pilot) tests, the average loading time was determined to be approximately 9997 s, with a standard deviation of $\sigma \approx 778$ s. The sample size was estimated using the formula specifying the required number of observations when comparing two means (formula 16), assuming a significance level of $\alpha = 0.10$ and a test power of 70%. Assuming a minimum difference between means of $\Delta = 600$ s as a practically relevant value—corresponding to approximately 10 minutes of crane operation (which represents about 6% of the average operation time)—the following result was obtained:

$$n = \frac{2\sigma^2(z_{1-\alpha/2} + z_{1-\beta})^2}{\Delta^2} \tag{16}$$

where:
n – required number of simulation repetitions,
σ – standard deviation of the analyzed variable (process completion time), based on pilot studies,
α – significance level of the statistical test,
β – probability of committing a Type II error,
$z_{1-\alpha/2}$ – quantile of the normal distribution corresponding to the assumed confidence level (for a two-tailed test),
$z_{1-\beta}$ – quantile of the normal distribution corresponding to test power (1−β),
Δ – minimum difference between means considered practically relevant from the standpoint of process efficiency.

The calculations show that with 16 repetitions, it is possible to detect differences in operation time of approximately 600 s while maintaining the assumed statistical test parameters. Therefore, 16 replications were adopted for each scenario in the subsequent analyses, which ensures sufficient result stability and enables a meaningful comparison of the quality of the analyzed algorithms with respect to process completion time. Aerodynamic values are treated secondarily—i.e., as an outcome of the container arrangement resulting from the loading process—and are analyzed independently for the results obtained in each iteration. The tables below present:

- crane operating time [s] before and after applying the algorithm improving aerodynamic parameters (Table 4),
- aerodynamic drag values [ft²] before and after applying the algorithm improving aerodynamic parameters (Table 5),

– differences in loading time and changes in aerodynamic drag for scenarios (Table 6).

A graphical representation of the results is provided in the plots (Figures 7 and 8).

Table 4. Results for scenarios 1A – 3C regarding crane operating time [s] before and after applying the algorithm improving aerodynamic parameters. Source: own elaboration

Rep.	1A		1B		1C	
	Before [s]	**After [s]**	**Before [s]**	**After [s]**	**Before [s]**	**After [s]**
1	9163	9163	8673	9352	8234	11533
2	7119	7119	7023	7650	6789	6789
3	9478	9478	8839	9479	8326	8971
4	13267	13267	11563	12440	10376	10376
5	8317	8317	8075	11854	7512	9781
6	7907	7907	6556	6556	6428	6428
7	8605	8605	9347	9347	8510	9260
8	10993	10993	9742	10640	9874	11130
9	6888	6888	8712	8712	7152	7290
10	7654	7654	7759	8230	7079	7480
11	8568	8568	7105	7420	6966	6966
12	7129	7129	7743	7870	7050	7470
13	8834	8834	7829	8470	7935	8900
14	7314	7314	9250	10130	7594	8100
15	9059	9059	9184	9860	8379	8970
16	6369	6369	6436	6690	6377	6920
avg	8541,50	8541,50	8364,75	9043,75	7786,31	8522,75
σ	1716,23	1716,23	1328,89	1692,92	1140,45	1596,75
p= 0,90	705,74	705,74	546,46	696,15	468,97	656,60
median	8442,50	8442,50	8374,00	9029,50	7553,00	8500,00
lower quartile Q1	7267,75	7267,75	7583,50	7815,00	7029,00	7209,00
upper quartile Q3	9085,00	9085,00	9200,50	9927,50	8339,25	9390,25
Rep.	**2A**		**2B**		**2C**	
	Before [s]	**After [s]**	**Before [s]**	**After [s]**	**Before [s]**	**After [s]**
1	16846	16846	15353	15805	15421	15421
2	12766	12766	11607	14208	11569	12835
3	14300	14300	12561	15965	13338	13574
4	14116	14116	11610	11610	10876	10876
5	14507	14507	12183	12183	12123	12123
6	12684	12684	11612	14650	11363	13200
7	12428	12428	10912	10912	9999	9999
8	12087	12087	11854	12980	11957	14350
9	12466	12466	9520	9520	10094	11440
10	14576	14576	12458	15810	13314	15890
11	11695	11695	9246	9246	9076	9920
12	13502	13502	12081	12740	10522	12540
13	12039	12039	12021	15130	9351	10008
14	13433	13433	14440	18670	10466	12240
15	10656	10656	11697	13950	8805	8805
16	13256	13256	11393	13670	10325	11950
avg	13209,81	13209,81	11909,25	13565,56	11162,44	12198,19
σ	1460,69	1460,69	1494,14	2515,11	1763,01	2013,20
p= 0,90	600,65	600,65	614,41	1034,25	724,97	827,85
median	13011,00	13011,00	11775,50	13810,00	10699,00	12181,50
lower quartile Q1	12342,75	12342,75	11553,50	12039,75	10070,25	10659,00
upper quartile Q3	14162,00	14162,00	12251,75	15298,75	11998,50	13293,50

Rep.	3A		3B		3C	
	Before [s]	**After [s]**	**Before [s]**	**After [s]**	**Before [s]**	**After [s]**
1	15344	15344	9890	12539	10527	13511
2	13891	13891	11181	12440	9630	12399
3	11135	11135	9672	11235	8639	10525
4	13860	13860	12512	13307	10758	13462
5	12974	12974	10745	11449	10429	12894
6	15065	15065	10936	13670	9761	12600
7	11142	11142	7723	9480	7063	9270
8	12515	12515	9539	11900	8589	11290
9	13769	13769	12488	15640	10869	14140
10	13949	13949	9668	11950	8842	11560
11	12312	12312	10617	13290	7778	9950
12	11899	11899	6887	8480	9718	12570
13	14533	14533	9054	11370	8972	11780
14	12864	12864	12997	16350	9859	12690
15	12778	12778	10876	13560	9412	12090
16	13864	13864	8139	10040	9955	12930
avg	13243,38	13243,38	10182,75	12293,75	9425,06	12103,81
σ	1261,02	1261,02	1724,30	2061,57	1062,95	1326,58
p= 0,90	518,55	518,55	709,05	847,75	437,10	545,51
median	13371,50	13371,50	10253,50	12195,00	9674,00	12484,50
lower quartile Q1	12464,25	12464,25	9417,75	11336,25	8791,25	11492,50
upper quartile Q3	13905,50	13905,50	10997,25	13370,25	10073,50	12903,00

Table 5. Results for variants 1A–3C regarding aerodynamic drag [ft²] before and after applying the algorithm improving aerodynamic parameters. Source: own elaboration

Rep.	1A		1B		1C	
	Before [ft^2]	**After [ft^2]**	**Before [ft^2]**	**After [ft^2]**	**Before [ft^2]**	**After [ft^2]**
1	2062,14	2062,14	2128,19	2044,22	2369,64	2222,48
2	2398,90	2398,90	2479,71	2401,42	2488,77	2428,07
3	2209,31	2209,31	2314,37	2230,35	2302,14	2211,31
4	2365,32	2365,32	2448,00	2350,81	2466,12	2405,97
5	2049,77	2049,77	2389,57	2291,69	2265,45	2175,90
6	2283,56	2283,56	2429,43	2370,18	2479,26	2418,79
7	2288,42	2288,42	2472,92	2288,42	2530,00	2305,87
8	2150,09	2150,09	2329,77	2221,19	2337,47	2184,19
9	2299,47	2299,47	2524,56	2299,47	2503,27	2328,36
10	2188,10	2188,10	2361,48	2217,31	2382,77	2212,37
11	2244,66	2244,66	2374,17	2268,41	2425,35	2244,66
12	2125,78	2125,78	2309,39	2130,76	2343,36	2128,26
13	2049,33	2049,33	2248,23	2076,56	2194,33	2050,71
14	2064,79	2064,79	2181,19	2101,33	2182,55	2090,13
15	2349,85	2349,85	2507,80	2387,09	2558,08	2436,01
16	1996,73	1996,73	2236,00	2016,57	2154,46	2061,15
avg	2195,39	2195,39	2358,42	2230,99	2373,94	2244,01
σ	128,53	128,53	117,97	124,38	128,26	130,92
p= 0,90	52,85	52,85	48,51	51,15	52,74	53,84
median	2198,71	2198,71	2367,83	2249,38	2376,21	2217,43
lower quartile Q1	2064,13	2064,13	2294,10	2123,40	2292,97	2163,99
upper quartile Q3	2291,18	2291,18	2454,23	2312,31	2481,64	2347,76

Rep.	2A		2B		2C	
	Before [ft²]	After [ft²]	Before [ft²]	After [ft²]	Before [ft²]	After [ft²]
1	2322,89	2322,89	2458,88	2375,66	2403,61	2344,99
2	2006,46	2006,46	2307,58	2015,88	2269,07	2071,40
3	2121,36	2121,36	2405,42	2130,53	2260,46	2176,50
4	2139,48	2139,48	2192,97	2139,48	2206,11	2152,30
5	2002,04	2002,04	2068,40	2017,95	2068,4	2017,95
6	2334,00	2334,00	2569,41	2346,74	2592,51	2373,95
7	2041,72	2041,72	2245,06	2190,31	2336,57	2279,58
8	2239,73	2239,73	2355,14	2234,78	2420,37	2243,50
9	1940,42	1940,42	2382,32	2324,21	2154,01	1984,08
10	2206,83	2206,83	2418,11	2251,71	2448,00	2211,72
11	1920,26	1920,26	2101,01	2049,77	2157,64	2044,42
12	2188,77	2188,77	2387,30	2318,57	2404,06	2205,25
13	2199,08	2199,08	2455,70	2217,50	2368,73	2287,94
14	2464,57	2464,57	2715,72	2464,57	2627,84	2480,49
15	2096,59	2096,59	2301,23	2130,27	2200,67	2147,00
16	2366,31	2366,31	2534,98	2402,35	2486,06	2406,55
avg	2161,91	2161,91	2368,70	2225,64	2337,76	2214,23
σ	158,56	158,56	168,30	138,94	160,27	144,14
p= 0,90	65,20	65,20	69,21	57,13	65,90	59,27
median	2164,13	2164,13	2384,81	2226,14	2352,65	2208,49
lower quartile Q1	2032,91	2032,91	2287,19	2130,47	2204,75	2128,10
upper quartile Q3	2260,52	2260,52	2456,50	2329,84	2427,28	2302,20

Rep.	3A		3B		3C	
	Before [ft²]	After [ft²]	Before [ft²]	After [ft²]	Before [ft²]	After [ft²]
1	2323,77	2323,77	2513,69	2388,33	2528,18	2339,39
2	1996,73	1996,73	2407,23	2060,00	2313,92	2034,99
3	2069,21	2069,21	2280,85	2093,37	2263,18	2170,95
4	2034,74	2034,74	2396,36	2120,22	2317,99	2051,29
5	2165,56	2165,56	2277,68	2159,81	2416,75	2202,47
6	2323,77	2323,77	2489,23	2354,91	2515,05	2364,93
7	1996,73	1996,73	2187,53	2041,85	2287,19	2033,05
8	2069,21	2069,21	2370,09	2104,79	2313,92	2100,71
9	2034,74	2034,74	2420,37	2061,54	2302,14	2057,12
10	2165,56	2165,56	2321,17	2217,14	2279,04	2210,87
11	2154,51	2154,51	2301,69	2201,45	2406,78	2264,45
12	2387,41	2387,41	2599,3	2460,66	2658,65	2434,78
13	2152,74	2152,74	2375,07	2195,46	2390,93	2198,77
14	2435,14	2435,14	2700,32	2489,64	2484,70	2313,92
15	2314,05	2314,05	2499,19	2356,53	2491,94	2335,95
16	2125,78	2125,78	2425,35	2186,38	2280,85	2143,39
avg	2171,85	2171,85	2410,32	2218,26	2390,70	2203,56
σ	142,60	142,60	129,55	146,78	116,22	128,80
p= 0,90	58,64	58,64	53,27	60,36	47,79	52,96
median	2153,63	2153,63	2401,80	2190,92	2354,46	2200,62
lower quartile Q1	2060,59	2060,59	2316,30	2101,94	2298,40	2089,81
upper quartile Q3	2316,48	2316,48	2491,72	2355,32	2486,51	2319,43

Table 6. Comparison of results for loading times and changes in aerodynamic drag. Source: own elaboration

Rep.	Avarage load time		Time difference		Avarage C_DA [ft^2]		C_DA difference	
	Before [s]	After [s]	[s]	[%]	Before [ft^2]	After [ft^2]	[ft^2]	[%]
1A	8541,5	8541,5	0,00	0,00	2195,389	2195,39	0,00	0,00%
1B	8364,75	9043,75	679,00	8,12%	2358,425	2230,99	-127,435	-5,71%
1C	7786,313	8522,75	736,44	9,46%	2373,94	2244,01	-129,93	-5,79%
2A	13209,81	13209,81	0,00	0,00	2161,907	2161,91	0,00	0,00%
2B	11909,25	13565,56	1656,31	13,91%	2368,702	2225,64	-143,062	-6,43%
2C	11162,44	12198,19	1035,75	9,28%	2337,757	2214,23	-123,527	-5,58%
3A	13243,38	13243,38	0,00	0,00%	2171,853	2171,85	0,00	0,00%
3B	10182,75	12293,75	2111,00	20,73%	2410,32	2218,26	-192,06	-8,66%
3C	9425,063	12103,81	2678,75	28,42%	2390,7	2203,56	-187,14	-8,49%

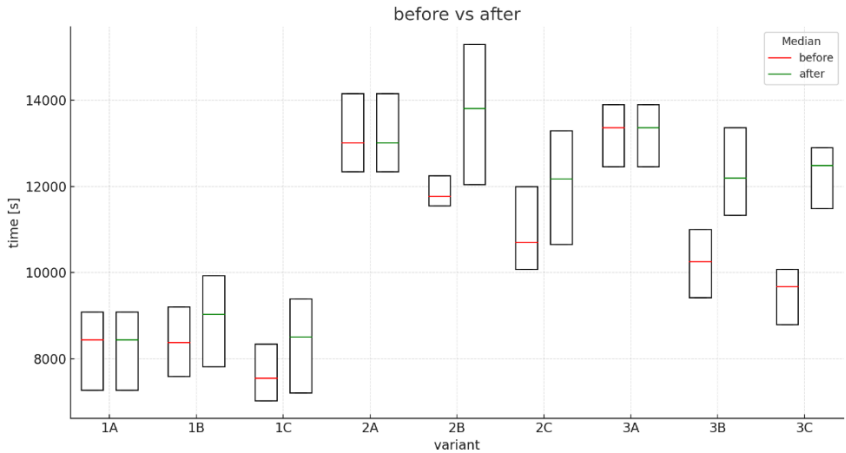


Fig. 7. Comparison of the average loading time for variants 1A–3C before and after aerodynamic parameter improvement. Source: own elaboration

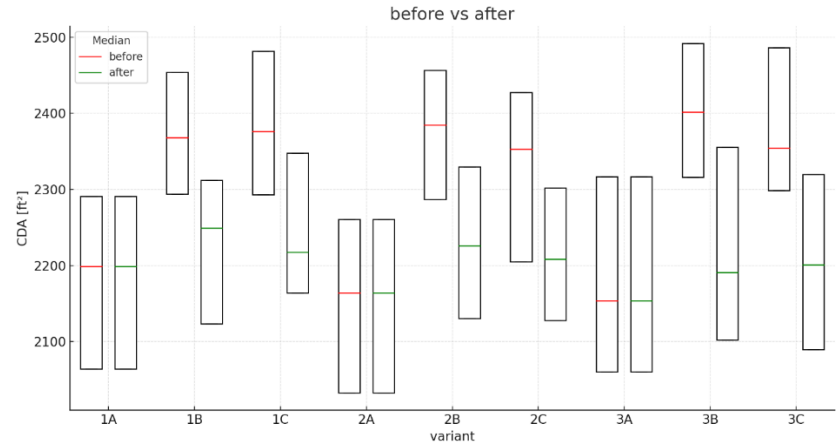


Fig. 8. Comparison of the average dynamic drag index for variants 1A–3C before and after aerodynamic parameter improvement. Source: own elaboration

6.3. Analysis of the results

When analysing the improvement of solution quality in the aerodynamic context, several fundamental relationships can be observed. These are mainly associated with:

- changes in the loading plan induced by procedures aimed at improving the aerodynamic properties of the trainset,
- the quality of the obtained solution before and after optimization,
- container configurations that either facilitate or limit optimization,
- analysis of configurations that are critical for solution quality in terms of aerodynamics.

The first aspect is primarily related to the manner in which the crane handles the cargo. Differences were observed between groups of variants that differed in the share of loads collected from specific terminal zones. The more complex the task (i.e., a larger search space for cargo—for example, in both the trackside lane and the storage yard, or only in the storage yard), the greater the potential for reconfiguring the initially obtained result in order to improve the aerodynamic properties of the trainset. For the simple tasks represented by variants 1A–1C, the improvement in aerodynamic parameters fluctuated around 5–6%. For variants 3A–3C, it already reached 6–9%. Moreover, in the more complex variants, crane operation time increased by over 25%. Algorithms based on distance minimization do not take into account the gaps arising between loads. Therefore, the larger the load search space, the more empty slots occur within the trainset, and the modification time required to correct this arrangement increases (e.g. the need to relocate a load from the last slot to a slot at the very front of the trainset).

A practical trade-off can therefore be clearly observed. For scenarios where dispersed container acquisition occurs (especially variants 3B and 3C), improving compactness resulted in up to approximately 20–28% longer crane operating time, while delivering up to 8–9% reduction in estimated aerodynamic drag. In situations where trains are operated on long-distance routes, even a small decrease in aerodynamic resistance translates into substantial traction energy savings, which may outweigh terminal-side operating time increases.

In view of the above, it is necessary to consider which aspect will provide greater energy benefits over the entire freight transport process in intermodal logistics—either the potential extension of crane operating time related to searching for an optimal placement of loading units, or accepting increased aerodynamic drag of the trainset resulting from a less favorable container configuration. An analysis of the energy balance of both approaches could constitute an important element in assessing the effectiveness of the proposed solutions.

Actual literature data indicate that RMG/RTG gantry cranes consume several kilowatt-hours per single handling cycle (approx. 3–8 kWh/TEU) (TNO, 2018). In contrast, electric freight trains are characterized by an average energy consumption of approximately 0.09–0.11 kWh/tkm (International Union of Railways [UIC], 2017). The share of aerodynamic drag in the total rolling resistance of freight trains reaches several tens of percent, and an improvement in aerodynamic parameters of even a few percent may translate into savings of several megawatt-hours of energy per single trip (Bulková et al., 2025).

For example, in variant 3C, the additional extension of crane operation time by 2679 s corresponds to an energy expenditure of approx. 74 kWh of electricity. At the same time, the obtained improvement in aerodynamic drag of 8.49% translates—assuming a typical intermodal trainset with a mass of approx. 2000 t and a transport distance of 500 km—into a reduction of traction energy demand by approx. 3000 kWh (Bulková et al., 2025). This means that the energetic cost of performing additional loading operations is more than forty times lower than the obtained energy benefit in the transport phase, and thus optimization of load unit arrangement in this variant is highly advantageous from an energy perspective.

The crane operating algorithms can be classified into two groups:

(1) Algorithms that limit the need for improving aerodynamic parameters. This refers to the algorithm based on slot priority (1). Due to the specific manner in which the crane searches for tasks to carry out, it serviced consecutive slots on the railcars in a predefined order (from the front to the end). As a result, the obtained solution almost always exhibited a compact arrangement of containers at the front of the trainset (Figure 9), with the potential occurrence of individual gaps at the end of the train. These gaps could not be eliminated due to the absence of

suitable containers located behind the empty slot (Figure 10).
(2) Heuristic-based algorithms (greedy algorithm and ant colony algorithm), which allow minimization of crane operation time, but typically generate solutions characterised by inferior aerodynamic parameters. For solutions based on algorithms 2 and 3, the occurrence of empty slots in the middle of the trainset was observed more frequently (Figure 11). In most cases, aerodynamic parameters of the trainset can be clearly improved by modifying the loading plan and incorporating, in addition to distance priority, also the priority of filling slots closer to the front of the train.

The critical factors influencing the aerodynamic drag index are, naturally, the length and location of empty slots on the railcars. A single empty slot positioned at the front of the trainset may generate an aerodynamic "penalty cost" comparable to that of several empty positions located at the end of the trainset. Much also depends on the nature of the loading task. Parameters such as the number of loads or the configuration of slots on railcars strongly affect solution quality in the aerodynamic context. Typically, the simplest algorithm (Algorithm 1) achieved the longest loading time but produced the lowest drag index. The remaining two algorithms, after container reconfiguration, often yielded values close to those obtained by Algorithm 1, although still rarely as low.

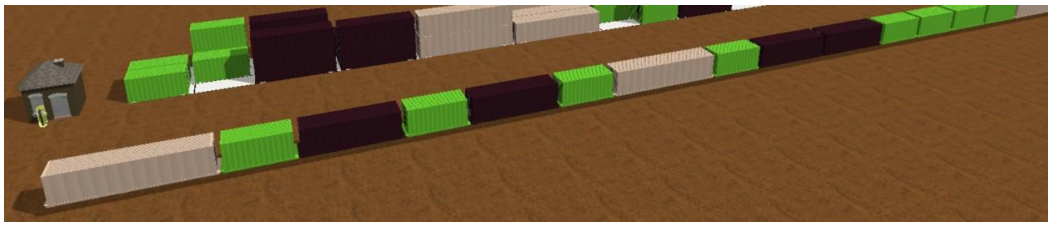


Fig. 9. Compact arrangement of containers at the front of the train (slot-priority algorithm). Source: own elaboration



Fig. 10. Example configuration of containers at the rear of the trainset (slot-priority algorithm). Source: own elaboration

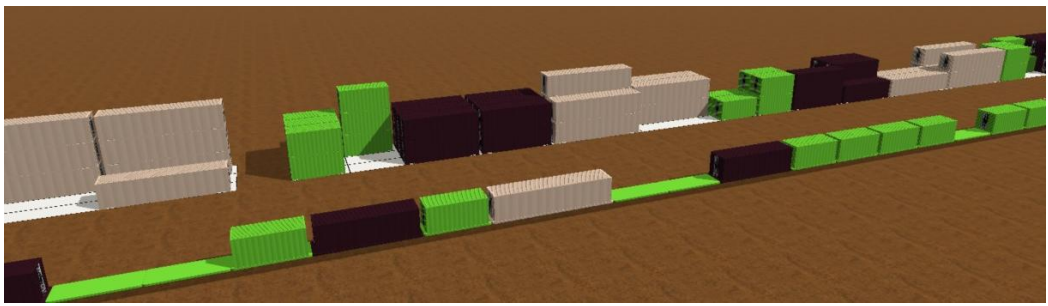


Fig.11. Empty slots in the middle of the trainset (greedy and ant colony algorithms). Source: own elaboration

The stochastic component cannot be ignored. In the analyzed measurement sample, it is clearly visible that both the susceptibility of the initial solution to aerodynamic improvement and the final solution quality in aerodynamic terms are strongly dependent on the particular case under consideration. Some randomly generated railcar and container configurations achieved a low drag index even without modifying the loading plan. Additionally, certain solutions exhibited significant aerodynamic improvement at very low additional operating time (on the order of only a few percent relative to the baseline). For others, despite extending the process duration by 20–30%, the aerodynamic results were not substantially better (improvement of only 1–2%). This may suggest that the decision to apply an aerodynamic improvement algorithm should be made individually, based on the analysis of the specific railcar–container configuration.

7. Summary

The research presented in this paper demonstrates that container arrangement on intermodal railcars has a measurable effect on aerodynamic drag, and consequently on the energy efficiency of intermodal freight transport. The novelty of the proposed approach lies in integrating loading-process optimization with the assessment of aerodynamic performance, which is rarely considered in operational decision-making at terminals. The introduction of a post-processing algorithm that reconfigures initially generated loading plans proved effective in reducing the estimated aerodynamic resistance of the train, in some cases by almost 9%, despite the additional handling effort.

The obtained results indicate that even relatively small reductions in aerodynamic drag may translate into substantial energy savings over long transport distances. For typical intermodal services operated on multi-hundred-kilometre routes, improved container compactness may reduce traction energy demand by several megawatt-hours per train movement. This highlights a tangible potential for reducing operational costs and environmental footprint solely through improved loading decisions.

However, the study also reveals important trade-offs. Terminals prioritize reduced crane operating time and higher throughput, whereas railway operators aim to minimize energy consumption during line haul. The results suggest that neither objective can be optimized independently and that a balanced compromise is required.

Future studies should expand the scope of the current modelling approach. Aerodynamic phenomena exhibit strong non-linearities, and their accurate representation requires validation beyond theoretical estimation. The most promising research direction is the integration of mathematical and simulation models with empirical measurements obtained either during actual train operations or using scaled experimental facilities such as wind-tunnel testing. Such combined approaches would allow further improvement of model fidelity and contribute to the development of decision-support tools capable of reconciling terminal-level operational efficiency with long-range energy performance of intermodal transport systems.

The proposed approach inherits several limitations resulting from the underlying modelling assumptions. Simulation experiments did not incorporate stochastic terminal disturbances (equipment availability, queueing, weather-related delays), whereas aerodynamic modelling used a simplified scalar indicator reflecting structural compactness of the consist. Moreover, crane paths were assumed deterministic. While these assumptions do not invalidate comparative results, they constrain the direct extrapolation of absolute performance values to field operation conditions.

Future research may extend this work in three directions: (I) refinement of aerodynamic modelling using CFD-verified penalty functions, (II) integration of drag estimation into the scheduling algorithm rather than post-processing optimization, and (III) introduction of multi-objective optimization, where crane time and aerodynamic performance are jointly evaluated.

References

1. Alicke, K., (2002). Modelling and optimization of the intermodal terminal Mega *Hub. OR Spectrum-Container transport and Automated Transport Systems*, 24, 307-323. Online: https://doi.org/10.1007/3-540-26686-0_13.
2. Arsene, S., Spiroiu, M.A., (2024). Study on the aerodynamics of freight trains used in container transport. *Acta Technica Napocensis*. 67(2), 787-796.
3. Ambrosino, D. Siri, S., (2014). Models for Train Load Planning Problems in a Container Terminal. Edycja: DE SOUSA, J. ROSSI, R. *Computer-based Modelling and Optimization in Transportation- Advances in Intelligent Systems and Computing*, 262, 15-25. https://doi.org/10.1007/978-3-319-04630-3_2.
4. Baker, C.J.. (2014). A review of train aerodynamics Part 2 - Applications. *Aeronautical Journal*. 118. 345-382. https://doi.org/10.1017/S0001924000009179.
5. Bruns, F. Knust, S., (2012). Optimized load planning of trains in intermodal transportation. OR Spectrum. 34(3). 511–533. https://doi.org/10.1007/s00291-010-0232-1.
6. Bulková, Z., Zitrický, V., Ľupták, V., Brabec, J., & Pečman, J. (2025). *Energy and emissions balance of modal shift in freight transport: A case study from the Central European region*. *Transportation Research Interdisciplinary Perspectives, 34*, 101656. https://doi.org/10.1016/j.trip.2025.101656
7. Corry, P. Kozan, E., (2008). Optimized load patterns for intermodal trains. *OR Spectrum*, 30, 721-750. https://doi.org/10.1007/s00291-007-0112-5.
8. Deng, R., Song, Z., Ren, H., Li, H., & Wu, T. (2022). Investigation on the effect of container configurations and forecastle fairings on wind resistance and aerodynamic performance of large container ships. *Engineering Applications of Computational Fluid Mechanics*, 16(1), 1279–1304. https://doi.org/10.1080/19942060.2022.2086177.
9. Dotoli, M. Epicoco, N. Falagario, M. Palma, D., (2013). A train load planning optimization model for intermodal freight transport terminals: a case study. *IEEE International Conference on Systems, Man, and Cybernetics*, 3597-3602. https://doi.org/10.1109/SMC.2013.613.
10. Dotoli, M. Epicoco, N. Seatzu, C., (2015). An improved technique for train load planning at intermodal rail-road terminals. *Procedings of 2015 IEEE 20th Conference on Emerging Technologies & Factory Automation (ETFA)*, https://doi.org/10.1109/ETFA.2015.7301580.
11. Flynn, D., Hemida, H., Baker. C., (2016). On the effect of crosswinds on the slipstream of a freight train and associated effects. *Journal of Wind Engineering and Industrial Aerodynamics*, 156, 2016, 14-28. https://doi.org/10.1016/j.jweia.2016.07.001.
12. Giappino, S., Melzi, S., Tomasini, G., (2018). High-speed freight trains for intermodal transportation: Wind tunnel study on the aerodynamic coefficients of container railcars. Journal of Wind Engineering and Industrial Aerodynamics, 175, 111-119. https://doi.org/10.1016/j.jweia.2018.01.047.
13. Heggen, H. Breakers, K. Caris A., (2018). Multi-objective approach for intermodal train load planning. *OR Spectrum*, 40(2), 341–366. https://doi.org/10.1007/s00291-017-0503-1.
14. Hungria, L.H., Soares, G., Mendes, F., (2019). Reducing the aerodynamic drag coefficient over double-stack trains L.H. *Rumo S.A.,* Curitiba, Paraná, Brazil.
15. Huo, X., Liu, T., Chen, Z., Li, W., & Gao, H. (2021). Effect of the formation type with different freight vehicles on the train aerodynamic performance. *Vehicle System Dynamics*, *60*(11), 3868–3896. https://doi.org/10.1080/00423114.2021.1981951.
16. International Union of Railways (UIC). (2017). *Railway Handbook 2017 – Energy consumption and CO_2 emissions*. IEA-UIC.
17. Kellner, M., Boysen, N., Fliedner, M., (2012). How to Park Freight Trains on Rail-Rail Transshipment Yards: The Train Location Problem. *Jena Research Papers in Business and Economics - Working and Discussion Papers*. 34. https://doi.org/10.1007/s00291-011-0246-3.
18. Kłodawski, M., Nehring, K., Jachimowski, R., Lipińska, J., (2024). The impact of the intermodal terminal operation strategy on container train loading duration. *Transport Problems*. 19(2). 163-176. https://doi.org/10.20858/tp.2023.19.2.13.

19. Lai, Y.-C., Barkan, C., Drapa, J., Ahuja, N., Hart, J., Narayanan, P., Jawahar, C., Kumar, A., Milhon, L., Stehly, M., (2007). Machine vision analysis of the energy efficiency of intermodal freight trains. *Proceedings of The Institution of Mechanical Engineers Part F-journal of Rail and Rapid Transit*. 221. https://doi.org/10.1243/09544097JRRT92.
20. Lai, Y.-C., Barkan, C., Onal, H., (2008). Optimizing the aerodynamic efficiency of intermodal freight trains. *Transportation Research Part E: Logistics and Transportation Review*. 44. 820-834. 10.1016/j.tre.2007.05.011.
21. Li, C. Burton, D. Kost, M. Sheridan, J. Thompson, M.C., (2017). Flow topology of a container train railcar subjected to varying local loading configuration. *Journal of Wind Engineering and Industrial Aerodynamics*, 169, 13-29. https://doi.org/10.1016/j.jweia.2017.06.011.
22. Li, W. Zhu X., (2019). Container Loading Optimization in Rail–Truck Intermodal Terminals Considering Energy Consumption. *Sustainability*, 11(8), 1-15. https://doi.org/10.3390/su11082383.
23. Majidian, H., Azarsina, F., (2018). Aerodynamic Simulation of A Containership to Evaluate Cargo Configuration Effect on Frontal Wind Loads. *China Ocean Eng.* 32, 196–205. https://doi.org/10.1007/s13344-018-0021-1.
24. Maleki, S., Burton, D., Thompson, M.C., (2019). Flow structure between freight train containers with implications for aerodynamic drag. *Journal of Wind Engineering and Industrial Aerodynamics*. 188, 194-206, https://doi.org/10.1016/j.jweia.2019.02.007.
25. Mosca, M. Mattera, L. Saccaro. S., (2018). Optimization of container operations at inland intermodal terminals. *International Journal of Transportation Systems*, 3, 21-29.
26. Nehring, K., Kłodawski, M., Jachimowski, R., Klimek, P., Vasek, R. (2021). Simulation analysis of the impact of container railcar pin configuration on the train loading time in the intermodal terminal. *Archives of Transport*, *60*(4), 155-169. https://doi.org/10.5604/01.3001.0015.6928.
27. Nehring, K., (2024). Wieloaspektowa metoda optymalizacji załadunku składu pociągu intermodalnego w terminalu lądowym (doctoral thesis). *Oficyna Wydawnicza Politechniki Warszawskiej*. p. 178.
28. Ng ManWo. Ng, Talley, W.K., (2020) Rail intermodal management at marine container terminals: Loading double stack trains. Transportation Research Part C: Emerging Technologies. 112, 252-259, https://doi.org/10.1016/j.trc.2020.01.025.
29. Opala M., (2021). Analysis of Safety Requirements for Securing the Semi-Trailer Truck on the Intermodal Railway Railcar. *Energies*. 14(20): 6539. https://doi.org/10.3390/en14206539
30. Öngüner, E., Henning, A., Fey, U., Wagner, C. (2020). Towards Aerodynamically Optimized Freight Railcars: An Experimental Study on Container Designs. In: Dillmann, A., Heller, G., Krämer, E., Wagner, C., Tropea, C., Jakirlić, S. (eds) New Results in Numerical and Experimental Fluid Mechanics XII. DGLR 2018. *Notes on Numerical Fluid Mechanics and Multidisciplinary Design*, 142. Springer, Cham. https://doi.org/10.1007/978-3-030-25253-3_42.
31. Östh, J., Krajnović, S., (2014). A study of the aerodynamics of a generic container freight railcar using Large-Eddy Simulation, Journal of Fluids and Structures, 44, 31-51, https://doi.org/10.1016/j.jfluidstructs.2013.09.017.
32. Said, G.A., E.A. El-Horbaty, E.M., (2015). An Optimization Methodology for Container Handling Using Genetic Algorithm. International Conference on Communication, *Management and Information Technology* (ICCMIT 2015), 65, 662-671. https://doi.org/10.1016/j.procs.2015.09.010.
33. Štastniak, P., Kurčík, P., Pavlík, A., (2018). Design of a new railway railcar for intermodal transport with the adaptable loading platform. *MATEC Web Conf.*, 235 (2018) 00030. https://doi.org/10.1051/matecconf/201823500030.
34. Quazi, A., Crouch, T., Bell, J., McGreevy, T., Thompson, M.C., Burton, D., (2021). A field study on the aerodynamics of freight trains. *Journal of Wind Engineering and Industrial Aerodynamics*. 209. 104463. https://doi.org/10.1016/j.jweia.2020.104463.
35. Rickett, T.G., Hart J.M., Edwards J.R., Kumar, A., Barkan, C.P.L., Ahuja, N. 2011. Monitoring the Aerodynamic Efficiency of Intermodal Train Loading Using Machine Vision. In: *Proceedings of Transportation Research Board 90th Annual Conference*. Washington, DC.

36. TNO. (2018). *Emissions of rail freight transport* (Report HT13Na). TNO.
37. Wang, L., Zhu, X., (2019). Container Loading Optimization in Rail–Truck Intermodal Terminals Considering Energy Consumption. *Sustainability*. 11(8). 2383. https://doi.org/10.3390/su11082383.
38. Zhang, D., Guo, Z. H., Ni, Y. Q., Chen, Z. W., Ao, W. K., Bordbar, A., & Zhou, F. R. (2023). Correlation between cargo properties and train overturning safety for a high-speed freight train under strong winds. *Engineering Applications of Computational Fluid Mechanics*, *17*(1). https://doi.org/10.1080/19942060.2023.2221308
39. Yang, M., Du, J., Li, Z., Huang, S., Zhou, D., (2017). Moving Model Test of High-Speed Train Aerodynamic Drag Based on Stagnation Pressure Measurements. *PLOS ON*E. 12. e0169471. https://doi.org/10.1371/journal.pone.0169471.